Dyes and Pigments 99 (2013) 966–971

Contents lists available at ScienceDirect

Dyes and Pigments

journal homepage: www.elsevier.com/locate/dyepig

A new fluorescent and colorimetric probe for trace hydrazine with a wide detection range in aqueous solution

Yiqun Tan, Jiancan Yu, Junkuo Gao, Yuanjing Cui, Yu Yang*, Guodong Qian*

State Key Laboratory of Silicon Materials, Cyrus Tang Center for Sensor Materials and Applications, Department of Materials Science & Engineering, Zhejiang University, Hangzhou 310027, China

ARTICLE INFO

Article history:
Received 24 April 2013
Received in revised form
29 July 2013
Accepted 14 August 2013
Available online 22 August 2013

Keywords:
Chemosensor
Fluorescent probe
Hydrazine
Fluorescence
Intramolecular charge transfer
Solvent effect

ABSTRACT

A new fluorescent and colorimetric probe based on the reaction and intramolecular charge transfer (ICT) effect is designed and synthesized. The probe responds rapidly toward hydrazine and exhibits distinct color changes from yellow to colorless, indicating its use as a color indicator for hydrazine. Moreover, the probe also shows a significant broad band fluorescence (410–700 nm) enhancement by ~120-fold after the addition of hydrazine. With a detection limit as low as 0.11 ppb, the probe can detect hydrazine in a wide concentration range because of the blunted sensing functional group. The contrast test shows almost no interruption from common elements in water, suggesting the high selectivity of this probe toward hydrazine. The theoretical calculation based on density functional theory (DFT) is also performed and two different ICT modes are found. This hydrazine probe would be a promising candidate applicable in environment protection, water treatment and safety inspection.

1. Introduction

Hydrazine (N_2H_4), as a highly reactive base and strong reducing agent, plays important roles in the synthesis of many chemicals, such as pharmaceuticals, pesticides, photography chemicals and various dyes [1–4]. In industry, it is often used as a chemical blowing agent and corrosion inhibitor for heating system [5]. Because of its highly explosive nature, hydrazine is also known as high energy fuel for propulsion systems in rocket and fuel cells [6,7]. However, with such a wide application in industry, hydrazine can easily cause environment pollution in the whole industrial process like manufacture, use and disposal [8,9]. In fact, hydrazine is toxic and readily absorbed by oral, dermal and inhalation uptake which can potentially lead to gene mutation and cancer [10–12]. In recent years, its damaging effect on lungs, kidneys, liver and central nervous systems has been discovered [13–15].

Due to its environment toxicity, detonable characteristic and widespread usage in industrial activities, development on reliable, sensitive and selective methods for the detection of trace hydrazine has attracted much attention [8,16–20]. Currently, a wide variety of measurement techniques have been developed, such as chromatography and electrochemical detection [10,21,22], which require either expensive experimental equipment or tedious operation processes. In recent years, fluorescence analysis system has been widely used to detect various targets because of its advantages such as high efficiency, sensitivity, selectivity, economy, simplicity and a large number of fluorescent sensors have been reported for various analytes [23–27]. However, researches toward developing small molecule fluorescent sensors for hydrazine have been rarely reported [9,28]. Nevertheless, these current reports still suffer from strong background signals, poor selectivity, high detection limit and narrow measurement range. To solve this problem, we develop a new fluorescent probe 2-(4-((4-(benzo[d]thiazol-2-yl)phenyl)ethynyl)benzylidene)malononitrile (BP) for hydrazine based on the ICT effect.

In this work, the photophysical properties, sensitivity and selectivity of BP are reported. Studies on the sensing mechanism are also carried out based on DFT and two different ICT modes are found.

2. Experimental section

2.1. Materials and measurements

4-Bromobenzaldehyde, 2-aminothiophenol, 2-methyl-3-butyn-2-ol and malononitrile were obtained from Aladdin® with the

* Corresponding authors. Tel.: +86 571 87952334; fax: +86 571 87951234.
E-mail addresses: yuyang@zju.edu.cn (Y. Yang), gdqian@zju.edu.cn (G. Qian).

0143-7208/$ – see front matter © 2013 Elsevier Ltd. All rights reserved.
http://dx.doi.org/10.1016/j.dyepig.2013.08.008

purity >98%. Cuprous iodide (CuI) and Bis(triphenylphosphine) palladium(II) dichloride ($Pd(PPh_3)_2Cl_2$) were purchased from Energy Chemical with the purity of 98%. All the solvents are provided by Sinopharm Chemical Reagent Co., Ltd with the purity >99.5%. All the solvents and reagents were used as received without further purification.

^{1}H NMR spectra were recorded in $CDCl_3$ on a 500 MHz Bruker Avance DMX500 spectrometer with tetramethylsilane (TMS) as an internal standard. Elemental analysis was performed using a Thermo Finnigan Flash EA1112 microelemental analyzer. Differential scanning calorimetry (DSC) was performed on a Netzsch Instruments 200 F3 at a heating rate of 10 K/min under nitrogen atmosphere. Fluorescence emission spectra and excitation spectra were obtained on a Hitachi F4600 fluorescence spectrophotometer. UV–vis absorption spectra were obtained using a Perkin–Elmer Lambda spectrophotometer. The Fluorescence decay curves were measured by an Edinburgh Instrument F900. Fluorescence quantum yield is measured with integrating sphere on Edinburgh Instrument F900.

All the theoretical calculations are performed based on DFT at the B3LYP/6–31G(d) level [29,30]. The solvent effect on molecular geometries is included by means of the polarizable continuum model (PCM) [31,32]. Based on the optimized geometry, all the molecular orbitals are calculated at the same level. All the calculations are performed in Gaussian 09 software [33].

2.2. Synthesis

2.2.1. 2-(4-Bromophenyl)benzothiazole (*1*)

4-Bromobenzaldehyde (0.46 g, 2.5 mmol) was stirred into a solution of 2-aminothiophenol (0.31 g, 2.5 mmol) in triethyl phosphate (25 mL). After 10 min, acetic acid (2.5 mL) was added into the solution and stirred for a further 10 min under temperature 60 °C. Lead(IV) acetate (1.5 g, 3.4 mmol) was added with rapid stirring. After stirred for a further 30 min, the solution was cooled to room temperature and extracted with CH_2Cl_2. The organic phase was collected and the solvent was evaporated. The resulting black solid was purified by chromatography using CH_2Cl_2 and petroleum (1:2) as eluent to obtain white solid **1** (0.46 g, 63%). ^{1}H NMR (500 MHz, $CDCl_3$): $\delta = 8.07$ (d, 1H), 7.96 (m, 2H), 7.91 (d, 1H), 7.63 (m, 2H), 7.50 (s, 1H), 7.38 (m, 2H). Anal. Calcd for $C_{13}H_8BrNS$: C, 53.81; N, 4.83; H, 2.78. Found: C, 53.81; N, 4.82; H, 2.76. Mp: 132.7 °C.

2.2.2. 4-(4-(Benzo[d]thiazol-2-yl)phenyl)-2-methylbut-3-yn-2-ol (*2*)

1 (1.44 g, 5 mmol), $Pd(PPh_3)_2Cl_2$ (0.14 g, 0.2 mmol), 2-methyl-3-butyn-2-ol (1.26 g, 15 mmol) and CuI (0.038 g, 0.2 mmol) were added into a mixture of Et_3N (2 mL) and toluene (8 mL) and refluxed for 12 h. The solution was evaporated and purified by chromatography using CH_2Cl_2 and EtOAC (20:1) as eluent, resulting in white crystal 2 (0.64 g, 44%). ^{1}H NMR (500 MHz, $CDCl_3$): $\delta = 8.06$ (d, 1H), 8.03 (d, 2H), 7.92 (d, 1H), 7.54 (t, 3H), 7.40 (s, 1H), 2.06 (s, 1H), 1.65 (s, 6H).

2.2.3. 2-(4-Ethynylphenyl)benzo[d]thiazole (*3*)

A mixture of **2** (0.59 g, 2 mmol) and KOH (0.56 g, 10 mmol) in toluene (10 mL) was refluxed for 2 h. The solution was then extracted with CH_2Cl_2, and the organic phase was combined and evaporated. The resulting black solid was purified by chromatography, using CH_2Cl_2 and petroleum (1:1) as eluent, afforded light yellow solid (0.42 g, 94%). ^{1}H NMR (500 MHz, $CDCl_3$): $\delta = 8.06$ (t, 3H), 7.92 (d, 1H), 7.62 (d, 2H), 7.52 (m, 1H), 7.41 (m, 1H), 3.23 (s, 1H). Anal. Calcd for $C_{15}H_9NS$: C, 76.57; N, 5.95; H, 3.86. Found: C, 76.48; N, 5.87; H, 4.14. Mp: 129.6 °C.

2.2.4. 4-((4-(Benzo[d]thiazol-2-yl)phenyl)ethynyl)benzaldehyde (*4*)

3 (0.94 g, 4 mmol) and 4-bromobenzaldehyde (0.74 g, 4 mmol) were solved into a mixture of Et_3N (4 mL) and toluene (16 mL). CuI (0.038 g, 0.2 mmol) and $Pd(PPh_3)_2Cl_2$ (0.14 g, 0.2 mmol) were stirred into the solution and heated at 90 °C for 12 h under argon atmosphere. The resulting solution was evaporated and purified by chromatography using CH_2Cl_2 and petroleum (1:1) as eluent to yield yellow solid **4** (0.98 g, 72%). ^{1}H NMR (500 MHz, $CDCl_3$): $\delta = 10.04$ (s, 1H), 8.12 (t, 3H), 8.61 (m, 3H), 7.69 (m, 4H), 7.52 (t, 1H), 7.42 (t, 1H). Anal. Calcd for $C_{22}H_{13}NOS$: C, 77.85; N, 4.13; H, 3.86. Found: C, 77.79; N, 4.18; H, 3.99. Mp: 138.6 °C.

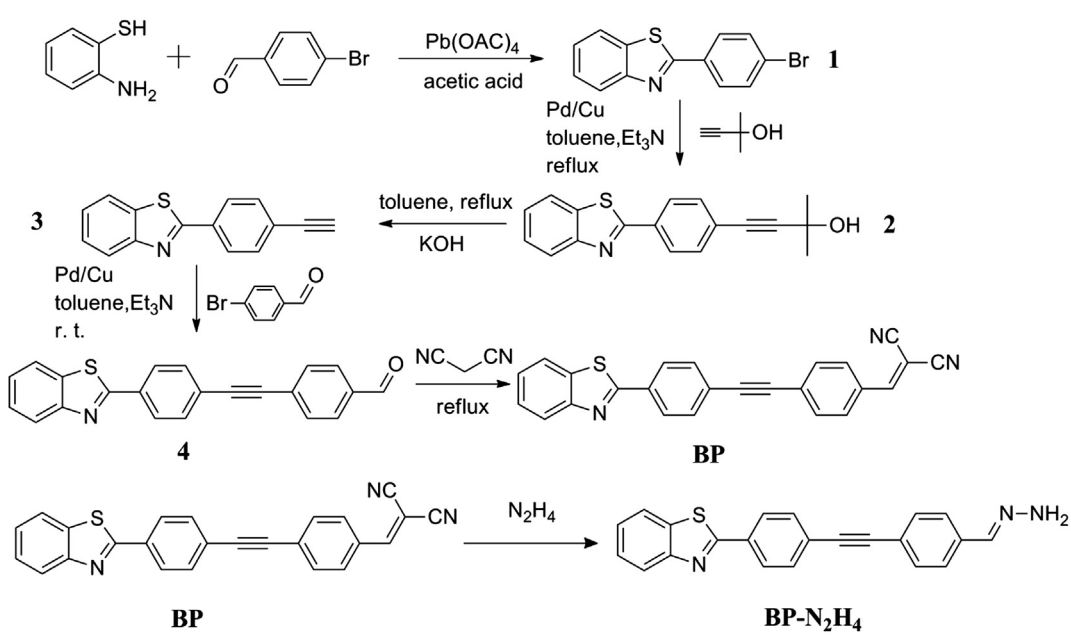

Scheme 1. Synthesis and proposed sensing mechanism of probe BP.

2.2.5. 2-(4-((4-(Benzo[d]thiazol-2-yl)phenyl)ethynyl)benzylidene)-malononitrile (BP)

4 (1.36 g, 4 mmol) was solved into EtOH (20 mL) and the solution was stirred at room temperature for 15 min. The mixture was then added with malononitrile (0.30 g, 4.53 mmol) and refluxed for 2 h. The resulting solution was evaporated and purified by chromatography using CH_2Cl_2 as eluent to yield yellow solid BP (1.30 g, 84%). ^{1}H NMR (500 MHz, $CDCl^3$): $\delta = 8.13$ (d, 2H), 8.10 (d, 1H), 7.93 (t, 3H), 7.75 (s, 1H), 7.69 (d, 4H), 7.53 (t, 1H), 7.43 (t, 1H). Anal. Calcd for $C_{25}H_{13}N_3S$: C, 77.50; N, 10.85; H, 3.38. Found: C, 77.62; N, 11.01; H, 3.52. Mp: 133.9 °C.

3. Results and discussion

3.1. Design and synthesis

ICT effect is a promising design strategy and has been widely applied in the development of various fluorescent probes [34–36]. Probes baring ICT effect are often composed by conjugation of donor and acceptor groups. Such a structure permits electrons transfer from the donor to the acceptor part, leading to both red-shift and intensity variation of fluorescence spectra [37–39]. Thereby, any changes in the donor or acceptor strength may cause spectra alteration, which could be used to recognize the targeted analytes. However, another interesting but easily neglected feature of ICT mechanism is the conjugation length induced blunting. The activity of the donor or acceptor would be reduced after combination with conjugated system, leading to the expansion of detection range [24,40]. By taking the advantage of this characteristic feature, a probe for hydrazine in a wide scope could be realized.

Herein, as shown in Scheme 1, benzothiazole was chosen as the electron acceptor because of its large conjugation system and electron dislocation, which might enhance the ICT effect [36,41]. As a strong electron withdrawing group and the sensing part for hydrazine, malononitrile is supposed to be replaced by hydrazine, leading to different intramolecular electron redistribution of the probe [28]. Thus both the absorption and fluorescence response can be expected. Moreover, because of the large conjugated system of the fluorophore, the reactivity of malononitrile, the sensing part, will be significantly weakened, resulting in the broadening of the detection range.

3.2. Photophysical properties

As shown in Fig. 1, a significant increase on the Stokes' shift with the increase on the solvent polarity in the order of toluene < THF < chloroform < acetone < acetonitrile can be seen from the absorption and fluorescence spectra of BP in various solvents, which is attributed to the (π–π^*) transition of the conjugated system in the fluorescence probe [42], indicating a strong ICT effect in the molecule during optical excitation [43–45]. The large Stokes' shift and the correlation between solvent polarity and emission color suggest the possible capability of BP as a fluorescent probe potentially applicable in environmental detection.

The main photophysical parameters of BP are listed in Table 1. With the increasing solvent polarity, the quantum yield of BP shows a moderate decrease, from 0.44 in toluene to 0.27 in acetonitrile, which can be ascribed to the relaxation of excited states caused by solvent molecules [46]. This phenomenon is a common character of fluorescent probes based on the ICT effect [47]. In the mixture of THF/water (1:1), the fluorescence of BP could hardly be observed for its poor quantum yield. Corresponding to the variations on quantum yield, the fluorescent lifetime of BH also shows a significant decrease with the increase of solvent polarity, while the molar extinction coefficients remain almost unchanged.

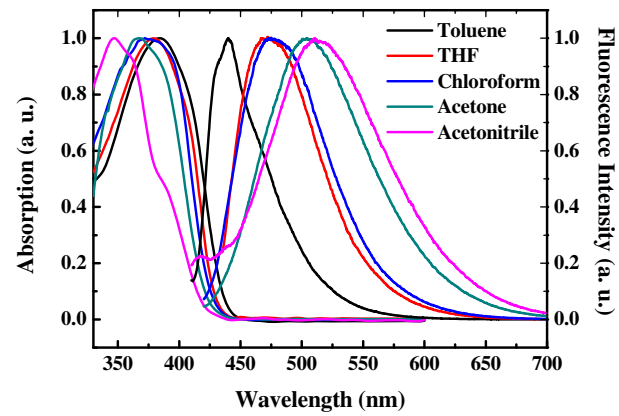

Fig. 1. Normalized absorption and relative fluorescence emission spectra of BP in various solvents at 10 μM.

3.3. Optical response

To test the practical utility of BP for the detection of hydrazine, the absorption response of BP toward hydrazine was first studied in the solution of THF. The probe showed almost intermediate color change from light yellow to colorless. The UV–vis spectroscopy showed a slight shift from 395 nm to 368 nm, depending on the gradual titration of hydrazine, as shown in Fig. 2. With the increase of hydrazine concentration, the absorption peak of BP at 395 nm decreased while that at 368 nm increased. The isosbestic point at 380 nm suggested the formation of a new substance, which might be ascribed to inhibition of the ICT effect in the probe molecules resulted from the substitution of malononitrile with hydrazine. The titration measurement reached saturation with the addition of 12 equiv. hydrazine, indicating a much broader detection range. This could be caused by the weakening of reaction activity resulting from the large conjugated system.

Probe BH exhibited weak fluorescence emission at 460 nm upon excitation at 395 nm in the solution of THF/water (1:1) at the

Table 1
Experimental photophysical properties of BP in different solvents.[a]

Sample	Solvent	ε^b, $\times 10^4$ L mol^{-1} cm^{-1}	Φ^c	Stokes' shift, nm	τ,[d] ns
BP	Toluene	3.6	44	71	$\tau_1 = 0.38$, $\tau_2 = 4.06$
	$CHCl_3$	3.8	42	90	$\tau_1 = 0.34$, $\tau_2 = 3.96$
	THF	3.6	41	90	$\tau_1 = 0.31$, $\tau_2 = 3.81$
	Acetone	3.7	29	145	$\tau_1 = 0.27$, $\tau_2 = 2.15$
	Acetonitrile	3.9	27	168	$\tau_1 = 0.27$, $\tau_2 = 1.99$
	THF/H_2O (1:1)[e]	3.5	–[f]	–	–
BP–N_2H_4[g]	THF/H_2O (1:1)	3.3	52	55	$\tau_1 = 0.57$, $\tau_2 = 4.75$

[a] The concentrations of BP is 10 μM in all the solvents except special stated.
[b] Molar distinction coefficient.
[c] Quantum yield of the sample.
[d] Fluorescence lifetime of BP and its reacted form of BP–N_2H_4.
[e] The concentration of BP in THF/H_2O is 10 nM.
[f] The signal is too small to be observed.
[g] The concentration of N_2H_4 is 120 nM.

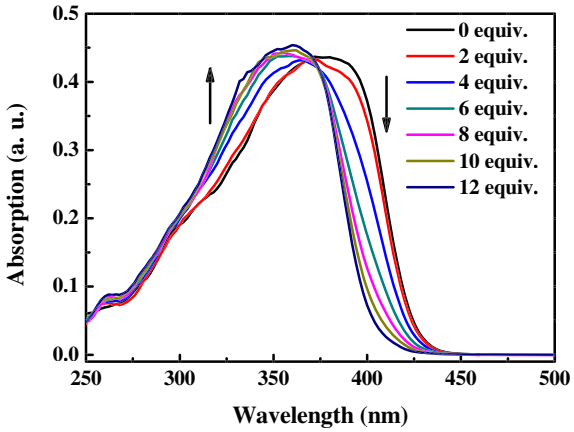

Fig. 2. Absorption spectra response of BP in THF at 10 nM toward hydrazine at different equivalent.

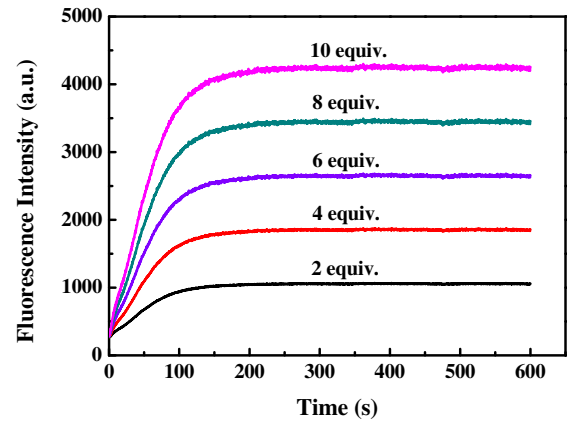

Fig. 4. Time related fluorescence intensity changes at 423 nm of BP in THF/water (1:1) at 10 nM upon titration of hydrazine at 2, 4, 6, 8 and 10 equiv. The excitation wavelength is 395 nm.

concentration of 10 nM. However, after the addition of hydrazine, drastic fluorescence enhancement (~100 times) at 423 nm could be observed. Further titration experiments on BP were also performed to test its fluorescence response. Upon the addition of hydrazine, gradual increase of fluorescence emission was exhibited. The probe showed two fluorescence emission bands at 423 and 480 nm respectively, and get to saturation with the addition of 12 equiv. hydrazine. The dependence of fluorescence intensity on hydrazine amount in the range of 60–120 nM could be well fitted linearly, as shown in Fig. 3. Thus, the detection limit (3σ/slope) could be as low as 3.4 nM (0.11 ppb), which was much lower than the regulated threshold limit values (10 ppb) from U.S. Environmental Protection Agency (EPA) [10].

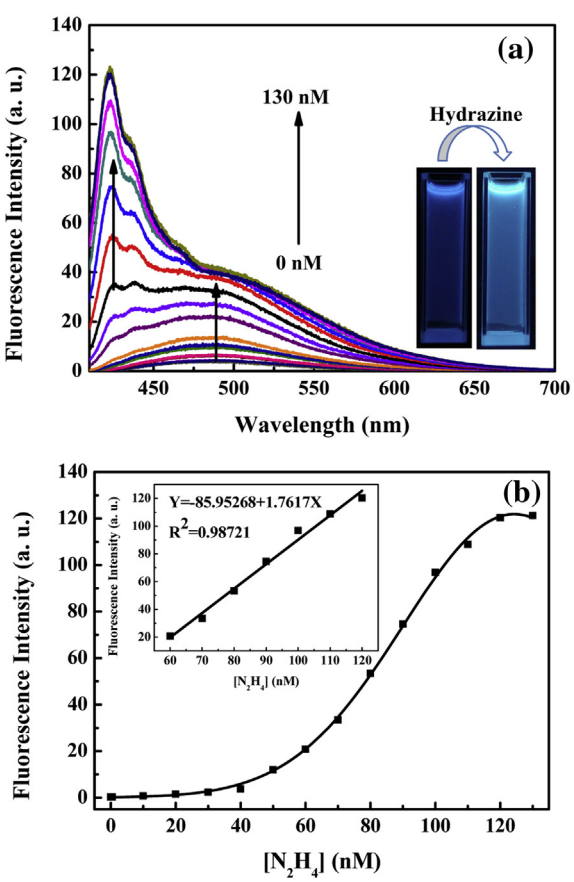

Fig. 3. Fluorescence spectra of BP in THF/water (1:1) at 10 nM excited at 395 nm upon titration of hydrazine.

To checkout its potential application in real-time detection, the time dependent fluorescence changes of BP with different amount of hydrazine were also studied, as shown in Fig. 4. The fluorescence intensity of BP at 423 nm increased until saturated in 2–3 min.

To testify the selectivity of probe BP toward hydrazine, various metal ions of environmental and biological interests such as Ni^{2+}, Ca^{2+}, Mg^{2+}, Al^{3+}, Zn^{2+}, K^{+}, Pb^{2+}, Co^{2+}, Cd^{2+}, Cr^{3+}, Cu^{2+} and Na^{+} were introduced to investigate their impact on the fluorescence response of BP. As shown in Fig. 5, the relative fluorescence intensity of BP remained almost unchanged after the addition of metal ions. They did not exert interference with fluorescence detection of hydrazine even at 10 equiv. either.

3.4. Theoretical calculations

To get insight into the sensing mechanism of BP toward hydrazine, computations on the probe before and after reacted with hydrazine are performed based on density functional theory (DFT). As shown in Fig. 6, electrons are mainly localized on the benzothiazole part at the ground state and transfer to the malononitrile accepter group after excitation, indicating stronger ICT effect. In this process, the benzothiazole group plays a role of donor because its

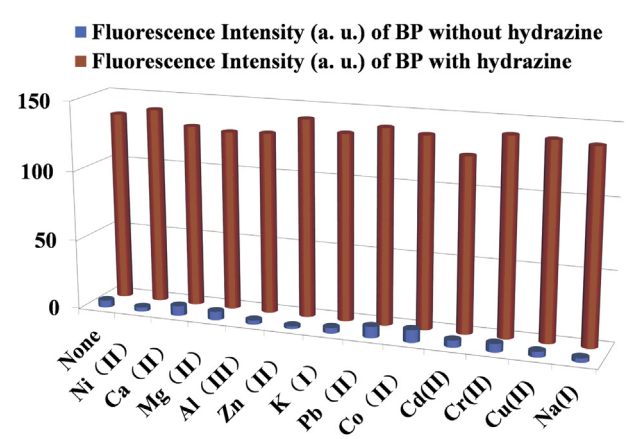

Fig. 5. The fluorescence intensity at 423 nm of BP at 10 nM with various competing ions upon excitation of 395 nm. The competing ions are at concentration of 1000 equiv. (10 μM) and hydrazine is 12 equiv.

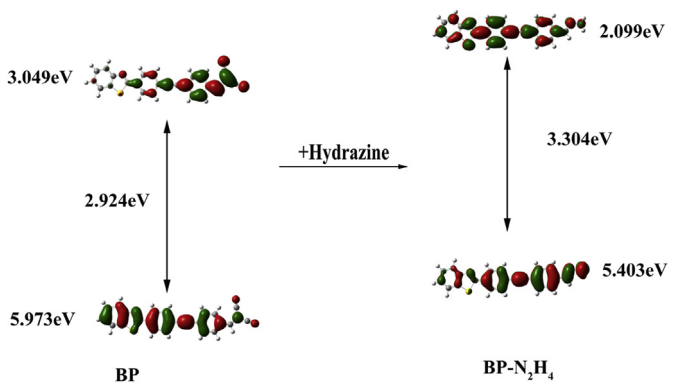

Fig. 6. HOMO–LUMO energy levels and the interfacial plots of the molecular orbitals for BP and its reacted form with hydrazine BP–N_2H_4.

electron-withdrawing ability is much lower than that of malononitrile group although it is actually electron-deficient. However, after reacted with hydrazine, the malononitrile group is substituted by electron-abundant hydrazine to form BP–N_2H_4, and the ICT direction is reversed. The electrons localized on the hydrazine part at the ground state and transfer to benzothiazole part at the excited state. Nevertheless, the ICT effect in BP–N_2H_4 is not as strong as that in BP, thus the absorption spectra of probe show significant blue-shift and an intense fluorescence enhancement can be observed.

4. Conclusion

In summary, we have designed and synthesized a new fluorescent probe for hydrazine. The probe exhibits high sensitivity and selectivity toward hydrazine with detection limit as low as 3.4 nM (0.11 ppb). Meanwhile, based on ICT effect and large conjugated system, detection in wide range of 6–10 equiv. can be realized. This probe could also applicant in the real-time detection for its rapid optical response to hydrazine, which could facilitate its application on the environmental protection, emergency process.

Acknowledgment

The authors gratefully acknowledge the financial support for this work from the National Natural Science Foundation of China (Nos. 51010002, 51272231 and 51229201), Natural Science Foundation of Zhejiang Province (No. LY12E02004) and the Fundamental Research Funds for the Central Universities.

References

[1] Ragnarsson U. Synthetic methodology for alkyl substituted hydrazines. Chem Soc Rev 2001;30(4):205–13.
[2] Narayanan SS, Scholz F. A comparative study of the electrocatalytic activities of some metal hexacyanoferrates for the oxidation of hydrazine. Electroanalysis 1999;11(7):465–9.
[3] Garrod S, Bollard ME, Nicholls AW, Connor SC, Connelly J, Nicholson JK, et al. Integrated metabonomic analysis of the multiorgan effects of hydrazine toxicity in the rat. Chem Res Toxicol 2005;18(2):115–22.
[4] Yamada K, Yasuda K, Fujiwara N, Siroma Z, Tanaka H, Miyazaki Y, et al. Potential application of anion-exchange membrane for hydrazine fuel cell electrolyte. Electrochem Commun 2003;5(10):892–6.
[5] Vieira LC, Lupetti KO, Fatibello O. Sweet potato (*Ipomoea batatas* (L.)Lam.) tissue as a biocatalyst in a paraffin/graphite biosensor for hydrazine determination in boiler feed water. Anal Lett 2002;35(14):2221–31.
[6] Wang J, Chen L. Hydrazine detection using a tyrosinase-based inhibition biosensor. Anal Chem 1995;67(20):3824–7.
[7] Serov A, Kwak C. Direct hydrazine fuel cells: a review. Appl Catal B 2010;98(1–2):1–9.
[8] Chen X, Xiang Y, Li Z, Tong A. Sensitive and selective fluorescence determination of trace hydrazine in aqueous solution utilizing 5-chlorosalicylaldehyde. Anal Chim Acta 2008;625(1):41–6.
[9] Choi MG, Hwang J, Moon JO, Sung J, Chang S-K. Hydrazine-selective chromogenic and fluorogenic probe based on levulinated coumarin. Org Lett 2011;13(19):5260–3.
[10] Umar A, Rahman MM, Kim SH, Hahn Y-B. Zinc oxide nanonail based chemical sensor for hydrazine detection. Chem Commun 2008;2:166–8.
[11] Liu J, Li Y, Jiang J, Huang X. C@ZnO nanorod array-based hydrazine electrochemical sensor with improved sensitivity and stability. Dalton Trans 2010;39(37):8693–7.
[12] Zhao Z, Zhang G, Gao Y, Yang X, Li Y. A novel detection technique of hydrazine hydrate: modality change of hydrogen bonding-induced rapid and ultrasensitive colorimetric assay. Chem Commun 2011;47(48):12816–8.
[13] Reilly CA, Aust SD. Peroxidase substrates stimulate the oxidation of hydralazine to metabolites which cause single-strand breaks in DNA. Chem Res Toxicol 1997;10(3):328–34.
[14] Mo J-W, Ogorevc B, Zhang X, Pihlar B. Cobalt and copper hexacyanoferrate modified carbon fiber microelectrode as an all-solid potentiometric microsensor for hydrazine. Electroanalysis 2000;12(1):48–54.
[15] Zelnick SD, Mattie DR, Stepaniak PC. Occupational exposure to hydrazines: treatment of acute central nervous system toxicity. Aviat Space Environ Med 2003;74(12):1285–91.
[16] Brown AB, Gibson TL, Baum JC, Ren T, Smith TM. Fluorescence-enhancement sensing of ammonia and hydrazines via disruption of the internal hydrogen bond in a carbazolopyridinophane. Sens Actuators B 2005;110(1):8–12.
[17] Ensafi AA, Rezaei B. Flow injection determination of hydrazine with fluorimetric detection. Talanta 1998;47(3):645–9.
[18] Collins GE, Rose-Pehrsson SL. Fluorescent detection of hydrazine, monomethylhydrazine, and 1,1-dimethylhydrazine by derivatization with aromatic dicarbaldehydes. Analyst 1994;119(8):1907–13.
[19] Collins GE, Rose-Pehrsson SL. Sensitive, fluorescent detection of hydrazine via derivatization with 2,3-naphthalene dicarboxaldehyde. Anal Chim Acta 1993;284(1):207–15.
[20] Thomas SW, Swager TM. Trace hydrazine detection with fluorescent conjugated polymers: a turn-on sensory mechanism. Adv Mater 2006;18(8):1047–50.
[21] Elder DP, Snodin D, Teasdale A. Control and analysis of hydrazine, hydrazides and hydrazones-genotoxic impurities in active pharmaceutical ingredients (APIs) and drug products. J Pharmaceut Biomed 2011;54(5):900–10.
[22] Batchelor-McAuley C, Banks CE, Simm AO, Jones TGJ, Compton RG. The electroanalytical detection of hydrazine: a comparison of the use of palladium nanoparticles supported on boron-doped diamond and palladium plated BDD microdisc array. Analyst 2006;131(1):106–10.
[23] Tan Y, Yu J, Cui Y, Yang Y, Wang Z, Hao X, et al. A novel 2,6-dicarbonylpyridine-based fluorescent chemosensor for Co^{2+} with high selectivity and sensitivity. Analyst 2011;136(24):5283–6.
[24] Tan Y, Yu J, Gao J, Cui Y, Wang Z, Yang Y, et al. A fluorescent pH chemosensor for strongly acidic conditions based on the intramolecular charge transfer (ICT) effect. RSC Adv 2013;3(15):4872–5.
[25] Yin S, Zhang J, Feng H, Zhao Z, Xu L, Qiu H, et al. Zn^{2+}-selective fluorescent turn-on chemosensor based on terpyridine-substituted siloles. Dyes Pigm 2012;95(2):174–9.
[26] Li Y, Wei F, Lu Y, He S, Zhao L, Zeng X. Novel mercury sensor based on water soluble styrylindolium dye. Dyes Pigm 2013;96(2):424–9.
[27] El Kaoutit H, Estévez P, Ibeas S, García FC, Serna F, Benabdelouahab FB, et al. Chromogenic and fluorogenic detection of cations in aqueous media by means of an acrylic polymer chemosensor with pendant rhodamine-based dyes. Dyes Pigm 2013;96(2):414–23.
[28] Fan J, Sun W, Hu M, Cao J, Cheng G, Dong H, et al. An ICT-based ratiometric probe for hydrazine and its application in live cells. Chem Commun 2012;48(65):8117–9.
[29] Becke AD. Density-functional thermochemistry. III. The role of exact exchange. J Chem Phys 1993;98(7):5648.
[30] Hehre WJ. Self-consistent molecular orbital methods. XII. Further extensions of Gaussian-type basis sets for use in molecular orbital studies of organic molecules. J Chem Phys 1972;56(5):2257.
[31] Tomasi J, Mennucci B, Cammi R. Quantum mechanical continuum solvation models. Chem Rev 2005;105(8):2999–3094.
[32] Cossi M, Rega N, Scalmani G, Barone V. Energies, structures, and electronic properties of molecules in solution with the C-PCM solvation model. J Comput Chem 2003;24(6):669–81.
[33] Frisch MJ, Trucks GW, Schlegel HB, Scuseria GE, Robb MA, Cheeseman JR, et al. Gaussian 09 RA. Wallingford, CT: Gaussian, Inc.; 2009.
[34] Kim HM, Cho BR. Two-photon probes for intracellular free metal ions, acidic vesicles, and lipid rafts in live tissues. Acct Chem Res 2009;42(7):863–72.
[35] Zhu B, Gao C, Zhao Y, Liu C, Li Y, Wei Q, et al. A 4-hydroxynaphthalimide-derived ratiometric fluorescent chemodosimeter for imaging palladium in living cells. Chem Commun 2011;47(30):8656–8.
[36] Nguyen DM, Frazer A, Rodriguez L, Belfield KD. Selective fluorescence sensing of zinc and mercury ions with hydrophilic 1,2,3-triazolyl fluorene probes. Chem Mater 2010;22(11):3472–81.
[37] Karton-Lifshin N, Albertazzi L, Bendikov M, Baran PS, Shabat D. "Donor–two-acceptor" dye design: a distinct gateway to NIR fluorescence. J Am Chem Soc 2012;134(50):20412–20.

[38] Delcamp JH, Shi Y, Yum JH, Sajoto T, Dell'orto E, Barlow S, et al. The role of pi bridges in high-efficiency DSCs based on unsymmetrical squaraines. Chem Eur J 2013;19(5):1819–27.
[39] Tan Y, Zhang Q, Yu J, Zhao X, Tian Y, Cui Y, et al. Solvent effect on two-photon absorption (TPA) of three novel dyes with large TPA cross-section and red emission. Dyes Pigm 2013;97(1):58–64.
[40] Zhou X, Su F, Tian Y, Youngbull C, Johnson RH, Meldrum DR. A new highly selective fluorescent K^+ sensor. J Am Chem Soc 2011;133(46):18530–3.
[41] Morales AR, Yanez CO, Zhang Y, Wang X, Biswas S, Urakami T, et al. Small molecule fluorophore and copolymer RGD peptide conjugates for ex vivo two-photon fluorescence tumor vasculature imaging. Biomaterials 2012;33(33):8477–85.
[42] Reichardt C. Solvatochromic dyes as solvent polarity indicators. Chem Rev 1994;94(8):2319–58.
[43] Wu J, Liu W, Ge J, Zhang H, Wang P. New sensing mechanisms for design of fluorescent chemosensors emerging in recent years. Chem Soc Rev 2011;40(7):3483–95.
[44] Mulliken RS. Molecular compounds and their spectra. II. J Am Chem Soc 1952;74(3):811–24.
[45] Mulliken RS. Molecular compounds and their spectra. III. The interaction of electron donors and acceptors. J Phys Chem 1952;56(7):801–22.
[46] Marini A, Munoz-Losa A, Biancardi A, Mennucci B. What is solvatochromism? J Phys Chem B 2010;114(51):17128–35.
[47] Lakowicz JR, Masters BR. Principles of fluorescence spectroscopy. J Biomed Opt 2008;13(2):029901–2 third ed.